Indoleamine 2,3-dioxygenase is a signaling protein in long-term tolerance by dendritic cells

Ursula Grohmann, Maria Teresa Pallotta, Ciriana Orabona, Claudia Volpi, Maria Laura Laura Belladonna, Roberta Bianchi, Giuseppe Servillo, Cinzia Brunacci, Mario Calvitti, Silvio Bicciato, et al.

Indoleamine 2,3-dioxygenase is a signaling protein in long-term tolerance by dendritic cells

Maria T. Pallotta,[1] Ciriana Orabona,[1] Claudia Volpi,[1] Carmine Vacca,[1] Maria L. Belladonna,[1] Roberta Bianchi,[1] Giuseppe Servillo,[2] Cinzia Brunacci,[2] Mario Calvitti,[1] Silvio Bicciato,[3] Emilia M.C. Mazza,[3] Louis Boon,[4] Fabio Grassi,[5] Maria C. Fioretti,[1] Francesca Fallarino,[1*] Paolo Puccetti,[1*] Ursula Grohmann[1*†]

Departments of [1]Experimental Medicine and Biochemical Sciences and [2]Clinical and Experimental Medicine, University of Perugia, 06126 Perugia, Italy. [3]Department of Biomedical Sciences, University of Modena and Reggio Emilia, 41100 Modena, Italy. [4]Bioceros BV, Utrecht 3584 CM, Netherlands. [5]Institute for Research in Biomedicine, Bellinzona, 6500 Switzerland

*These authors share senior authorship.

Author Information Correspondence should be addressed to U.G. (ugrohmann@tin.it).

Manuscript details

Abstract—109 words (Title, 12)

Number of words of text, <4,000

Number of figures and individual parts—8 figures

Online Methods—1,322 words.

Supplementary Information—Supplementary Figures 1 to 12 with Legends.

Regulation of tryptophan metabolism by indoleamine 2,3-dioxygenase (IDO) in dendritic cells (DCs) is a highly versatile modulator of immunity. In inflammation, interferon γ (IFN-γ) is the primary IDO inducer to prevent hyperinflammatory responses, yet the enzyme is also responsible for longer-term self-tolerance effects. Here we show that treatment of mouse plasmacytoid DCs (pDCs) with transforming growth factor β (TGF-β) conferred regulatory effects on IDO that were mechanistically separable from its enzymic activity. We reveal that IDO is involved in intracellular signaling events responsible for self-amplification and maintenance of a stably regulatory phenotype in pDCs. Thus IDO has a tonic, non-enzymic function that contributes to TGF-β–driven tolerance in non-inflammatory contexts.

Immune regulation is a highly evolved biologic response capable of fine-tuning inflammation and innate immunity, but also of modulating adaptive immunity and establishing tolerance to self[1,2]. Amino acid catabolism is an ancestral survival strategy that can additionally control immune responses in mammals[3]. Several metabolic enzymes are known to possess a second function, which allows them to meet additional functional challenges and needs inside the cell[4]. Three distinct enzymes, namely tryptophan 2,3-dioxygenase (TDO; confined to the liver), IDO (also referred to as IDO1), and the IDO paralogue indoleamine 2,3-dioxygenase–2 (IDO2) catalyze the same rate-limiting step of tryptophan (Trp) catabolism along a common pathway, which leads to Trp starvation and the production of Trp metabolites collectively known as kynurenines[5-7]. However, IDO alone is recognized as an authentic regulator of immunity in a variety of physiopathologic conditions, including pregnancy, infection, allergy, autoimmunity, chronic inflammation, transplantation, and immuno-escaping tumoral mechanisms[8,9].

Normally expressed at low basal levels, IDO is rapidly induced by IFN-γ in DCs[8-10]. The IFN-γ–IDO axis is considered to be a phylogenetically conserved mechanism of restricting microbial growth and avoiding potentially harmful (hyper) inflammatory responses in the host[11]. However, its regulatory function in pregnancy and long-term prevention of immunopathology have been unclear[8-10]. Autocrine or paracrine signaling through transforming growth factor β (TGF-β) can also induce long-term, IDO-dependent effects[12]. The TGF-β–IDO axis was shown to mediate

durable regulatory functions, with a primary role in the generation and maintenance of regulatory T (T_{reg}) cells[13].

Functional flexibility and fostering of T_{reg} responses are features typical of $CD11c^{low}B220^{high}$ plasmacytoid DCs (pDCs), which are capable of activating but also suppressing both inflammatory or innate responses and adaptive immunity[14-17]. Although different forms of immunosuppressive mechanisms are exploited by pDCs in distinct environmental conditions[15], IDO is one of the key molecular components responsible for pDC-induced tolerogenesis[9,18]. Thus, depending on a specific physiopatological context, IDO and pDCs will exhibit adaptable and integrated modes of immune control. Here we provide evidence that IDO expressed by pDCs can meet different environmental needs, and in particular, that locally produced cytokines can change its main function from an intense but short course of Trp degradation (e.g., in IFN-γ–dominated innate or inflammatory responses) to a TGF-β–driven, self-maintaining form of intracellular signaling activity, which—independently of tryptophan degradation—contributes to sustaining a stably regulatory phenotype in pDCs, as required by tolerance mechanisms.

RESULTS

IDO regulatory functions independent of its catalytic activity

We compared the effects of pDC conditioning with either IFN-γ or TGF-β in cocultures established with naïve $CD4^+CD25^-$ T lymphocytes. To identify IDO-dependent effects of either cytokine, groups of pDCs were transfected with *Ido1* or *Ido2* small interfering RNA (siRNA) (**Supplementary Fig. 1**) or treated with 1-methyltryptophan (1-MT), an inhibitor of IDO's enzymic activity, prior to cytokine conditioning. We assessed the proliferation, apoptosis, percentage of cells expressing CD4 and the transcription factor Foxp3, as well as the cytokine profile after 1–4 d of culture. pDC pretreatment with IFN-γ but not TGF-β induced a reduction in the proliferation (**Fig. 1a** and **Supplementary Fig. 2**) and an increase in the rate of apoptosis (**Fig. 1b** and **Supplementary Fig. 3**) of $CD4^+$ cells, as compared to cocultures established with untreated pDCs. In contrast, TGF-β pretreatment of pDCs induced a higher percentage of $Foxp3^+$ cells in the $CD4^+$ cell population (**Fig. 1c** and **Supplementary Fig. 4**), which was also characterized by marked suppressive activity *in vitro* (**Fig. 1d**). Supernatants from cocultures established with TGF-β– but not IFN-γ–treated pDCs contained higher amounts of IL-27, but less IL-6, as compared to controls (**Fig. 1e**). However, while secreted cytokines could be found in culture supernatants, TGF-β was present in a large latent complex or as a biologically active cell surface molecule[13], as demonstrated by cellular staining for the cytokine (**Fig. 1f**), and Real-Time PCR data (**Supplementary Fig. 5**). TGF-β stimulation also induced TGF-β expression in pDCs from wild-type but not from $Ido1^{-/-}$ mice (**Fig. 1f** and **Supplementary Fig. 5**). Although *Ido1* (but not *Ido2*) silencing abrogated the *in vitro* effects of both IFN-γ and TGF-β, the use of 1-MT prevented the IFN-γ–dependent but not the TGF-β–mediated immunomodulatory effect on the pDCs (**Fig. 1a-e**). Therefore, TGF-β induces TGF-β and IDO-dependent regulatory functions in pDCs *in vitro* that do not require IDO's catalyst function.

TGF-β induces IDO regulatory functions in pDCs *in vivo*

In *in vivo* experiments, female mice were sensitized with the $H\text{-}2D^b$–restricted HY peptide (containing the immunodominant epitope of the mouse male-specific minor transplantation antigen) presented by $CD11c^{high}$ conventional DCs (cDCs), administered alone or in combination with a minority fraction of potentially

regulatory pDCs, either untreated or pretreated with IFN-γ or TGF-β. After priming, reactivity was assessed at 2 wk by intrafootpad challenge with the HY peptide in the absence of DCs, according to an established protocol measuring induction of immune reactivity *vs.* tolerance[19,20]. The priming ability of cDCs was not affected by the presence of untreated pDCs[20], yet co-sensitization with pDCs pretreated with either cytokine caused suppression of HY-specific reactivity, an effect abrogated by *Ido1* but not *Ido2* silencing in the pDCs used for sensitizing hosts. However, 1-MT selectively blocked the immunosuppressive effect induced by pDC pretreatment with IFN-γ but not TGF-β, and the immunosuppressive effect of pDCs was abolished by neutralization of endogenous TGF-β (**Fig. 2a**). A conspicuous lymphomononuclear infiltrate was observed in the experimental footpads of skin test-positive mice (**Fig. 2b**), whose popliteal lymph nodes expressed a T_H1-type response dominated by the production of IFN-γ (**Fig. 2c**). A significant increase in Foxp3-expressing $CD4^+$ cells was observed in the popliteal lymph nodes, but not spleens and mesenteric lymph nodes, of skin test-negative mice selectively treated with TGF-β-conditioned pDCs (**Fig. 2d** and **Supplementary Figs. 6** and **7**). These data suggested that TGF-β induces IDO-dependent immunoregulatory effects in pDCs *in vivo* that are distinct in nature from those induced by IFN-γ and are independent of the catalyst function of the IDO protein.

TGF-β activates SHPs in pDCs

The immunoreceptor tyrosine-based inhibitory motifs (ITIMs) are known to signal via recruitment and activation of Src homology 2 domain phosphotyrosine phosphatase 1 (SHP-1), SHP-2, and inositol polyphosphate-5-phosphatase D (SHIP)[21,22]. A prototypic ITIM has the I/V/L/SxYxxL/V/F sequence[23,24], where x denotes any amino acid and Y the phosphorylable tyrosine. In the presence of inflammatory stimuli, phosphorylated ITIMs bind suppressor of cytokine signaling 3 (SOCS3), which, in turn, mediates proteasomal degradation of ITIM-bearing molecules[25,26]. Mouse IDO possesses two putative ITIMs that, in the presence of proinflammatory IL-6, mediate SOCS3-dependent proteasomal degradation of the enzyme[27]. Alignment of human, dog, rat, and mouse IDO proteins indicates that the putative ITIMs in mouse IDO (hereafter referred to as ITIM1 and ITIM2) are well conserved in mammals and are located at sites distant from the catalytic domain. In contrast, in mouse and human

IDO2, as well as in their chicken and fish counterparts, only the putative ITIM2 is present, due to a tyrosine substitution with phenylalanine in ITIM1.

To investigate whether IDO displays ITIM-mediated signaling ability, we first evaluated the kinetics of ITIM phosphorylation in IDO as well as the expression of SHP-1, SHP-2, and SHIP phosphatases in pDCs treated with TGF-β or IFN-γ. Using an antibody raised to a peptide containing the tyrosine phosphorylated form of IDO ITIM2 (pITIM2; p-IDO) (**Supplementary Fig. 8**), we found that, as early as 30 min following treatment, TGF-β, but not IFN-γ, induced the appearance of pITIM2–containing molecules in the range of the known IDO protein size, i.e., 42–45 kDa (**Fig. 3a**). No binding by anti-pITIM2 antibody could be observed in pDC lysates from *Ido1*$^{-/-}$ mice subjected to TGF-β or IFN-γ treatment (data not shown). The expression of genes coding for SHP-1 (*Ptpn6*), SHP-2 (*Ptpn11*), and SHIP (*Inpp5d*) increased at 16–24 h in response to TGF-β but not IFN-γ (**Fig. 3b**). In contrast, pDC treatment with IL-6 invariably led to a reduced expression of these genes (data not shown).

To verify whether the pITIMs in IDO could represent true docking sites for phosphatases, biotinylated peptides containing phosphorylated or unphosphorylated IDO ITIM1 or ITIM2 sequences were used to pull-down SHP-1, SHP-2, and SHIP. Lysates from P1 tumor cells (constitutively expressing high levels of phosphatases) and pDCs (incubated with TGF-β for 24 h) were exposed to the biotinylated peptides and immunoprecipitated with streptavidin-agarose (**Fig. 3c**). SHIP binding was not detectable under any conditions. In contrast, SHP-1 and SHP-2 bound pITIM1 and pITIM2, but not their unphosphorylated counterparts, in both cell types. In co-immunoprecipitation experiments, SHP-1 and SHP-2 were barely detectable in IDO immunoprecipitates obtained from lysates of pDCs in the absence of cytokine treatment (**Fig. 3d**). Yet, SHP-1 and SHP-2 co-immunoprecipitation efficiency increased in lysates of pDCs treated with TGF-β for 24 h. In addition, significant levels of tyrosine phosphatase activity were found in IDO co-immunoprecipitates from pDCs treated with TGF-β, but those effects were markedly suppressed by pDC transfection with *Ptpn6* or *Ptpn11* siRNA, or by treatment with stibogluconate (a specific SHP-1 inhibitor) prior to TGF-β treatment (**Fig. 3e** and **Supplementary Fig. 9**).

We next assessed the ratio of bound to total IDO in IDO-transfected pDCs which, unlike unmanipulated cells, can provide sufficient amounts of co-immunoprecipitate. Bound IDO was calculated as the difference between total IDO and residual IDO protein after immunoprecipitation with anti-SHPs. The amounts of IDO in whole cell lysates were determined by immunoblotting with anti-IDO before (total amount) and after immunoprecipitation (residual amount). In two independent experiments, the percentage of reduction in IDO/β-tubulin ratio in TGF-β–treated pDCs after co-immunoprecipitation with anti–SHP-1/2 were 23.8% and 23.2%, respectively (data not shown). Therefore, approximately one-fourth of total IDO appeared to have co-immunoprecipitated with SHP-1 or SHIP-2—and thus to be phosphorylated—in pDCs treated with TGF-β.

Studies with P1 transfectants expressing IDO mutants lacking the ITIM1 tyrosine, the ITIM2 tyrosine, or the histidine residue required for catalytic activity revealed that both ITIMs, but not the catalytic site, were required for binding and activation of tyrosine phosphatases, an ability unshared by IDO2 (**Fig. 3f,g**). These data suggested that, in pDCs, TGF-β induces phosphorylation of IDO ITIMs, up-regulation of SHP-1 and SHP-2, and thus favors the formation of IDO–SHP-1/SHP-2 complexes and the activation of SHP-1 and SHP-2 phosphatase activity.

Fyn-dependent phosphorylation of IDO ITIMs

TGF-β modulates numerous diverse cellular phenotypes in distinct types of cell via Smad-dependent and -independent pathways[13]. Smad-independent signaling includes the phosphoinositide-3-kinase (PI3K) pathway, which might link TGF-β with noncanonical NF-κB[13]. We used inhibitors of all Smad downstream effects (SIS3) and a PI3K specific inhibitor (LY294002) to investigate the effect of Smad-dependent and Smad-independent TGF-β–induced pathways on both IDO phosphorylation (**Fig. 4a**) and transcriptional expression of *Ptpn6* (**Fig. 4b**). The results showed that IDO phosphorylation (which happens early) was Smad-independent but PI3K-dependent, whereas the later induction of *Ptpn6* was contingent on both Smad and PI3K.

We looked for the kinase responsible for phosphorylation of the critical tyrosines in IDO ITIMs. To gain preliminary insight, we searched the pDC gene expression profiles from public datasets focusing on Src kinases known to mediate surface receptor-dependent tyrosine phosphorylation of intracellular target proteins[28].

Profile analysis indicated that, among a few possibilities including *Sykb*, *Blk*, *Frk*, *Zap70*, *Fgr*, *Fyn*, *Hck*, *Lck*, *Lyn*, *Src*, *Yes1*, and *Csk*, the most widely represented kinase in naive mouse pDCs was the *Fyn* gene product (**Fig. 4c,d**). Consistent with these data, we found that Fyn was expressed very abundantly in pDCs, such that TGF-β increased protein expression only marginally (**Fig. 4e**). To investigate any functional role of Fyn in TGF-β–induced phosphorylation ITIM tyrosines in IDO, we pretreated pDCs with the Fyn inhibitor PP2 or the control PP3 molecule as well as with an inhibitor of Syk, the major kinase related to ITAM or ITIM tyrosine phosphorylation in other cell types[29]. Immunoblot analysis demonstrated that selective inhibition of Fyn function greatly impaired IDO phosphorylation (**Fig. 4f**). These data demonstrate that the TGF-β–induced association of IDO ITIMs with SHP molecules requires Fyn-dependent phosphorylation of IDO, while induction of SHP expression is mediated through a combination of Smad-dependent and -independent mechanisms.

TGF-β–IDO–SHP axis activates the noncanonical NF-κB pathway

We sought to gain insight into the signaling circuitry and the downstream targets activated by the TGF-β–IDO–SHP axis in pDCs. In splenocytes, SHP-1 inhibits IRAK1 (interleukin-1 receptor-associated kinase 1) and tips the balance of canonical *vs.* noncanonical NF-κB activation in favor of the latter, resulting in upregulated type I IFN production[30,31]. We evaluated the activation of canonical *vs.* noncanonical NF-κB and the production of IFN-α and IFN-β in pDCs in response to TGF-β and IFN-γ. As previously reported[12], TGF-β induced phosphorylation of the IκB kinase α (IKKα) at 30 min, which is known to be indispensable for the activation of the noncanonical NF-κB pathway. There was no increase in the phosphorylation of IκB kinase β (IKKβ), which is pivotal in the canonical NF-κB pathway (**Fig. 5a**). In contrast, IFN-γ induced low, yet detectable, phosphorylation of both kinases. In addition, we found a selective increase in the nuclear translocation of p52 and RelB (both functional markers of noncanonical NF-κB) in pDCs treated for 30–60 min with TGF-β, whereas IFN-γ had negligible effects (**Fig. 5b**). Significant levels of IFN-α (**Fig. 5c**) and IFN-β (data not shown) were found in culture supernatants obtained by treating pDCs for 24 h with TGF-β, but not with IFN-γ. Silencing either *Ptpn6* or

Ptpn11 markedly impaired nuclear translocation of p52 (**Fig. 5b**) and IFN-α production (**Fig. 5c**) in TGF-β-treated pDCs. In addition, silencing of both *Ptpn6* and *Ptpn11*, *Ido1*, or *Chuk* alone (encoding IKKα)[20] abrogated IFN-α (**Fig. 5c**) and IFN-β production (data not shown) in TGF-β-treated pDCs. No such effect was obtained by silencing *Ido2* or *Ikbkb* (encoding IKKβ) or by treating cells with 1-MT (**Fig. 5c**). Silencing of *Irak1* resulted in a marked upregulation of IFN-α production (**Fig. 5c**) in pDCs treated for 24 h with TGF-β, consistent with the previously reported inhibitory effect of IRAK1 on type I IFN release[30]. In co-immunoprecipitation experiments the basal association of IRAK1 with SHPs was enhanced by TGF-β (**Fig. 5d**). Thus SHP-1 favors TGF-β-dependent activation of the noncanonical NF-κB pathway and IFN-α production in pDCs, via pathways involving IRAK1.

IDO phosphorylation initiates a circuitry of downstream events

Next, we used wild-type pDCs pretreated with *Ptpn6*-*Ptpn11*, *Chuk*, or *Ikbkb* siRNA or pDCs purified from *Ifnar*$^{-/-}$ mice (i.e., lacking the gene encoding the IFN-α/β receptor) to investigate the role of IDO-dependent pathways in TGF-β signaling. In pDC-T cell cocultures, lack of *Ptpn6*-*Ptpn11*, *Chuk*, or *Ifnar,* but not of *Ikbkb*, in pDCs greatly impaired the capacity of TGF-β–treated pDCs to induce $CD4^+Foxp3^+$ cells (**Fig. 6a** and **Supplementary Fig. 10**) and decrease IL-6 production (**Fig. 6b**). Lack of *Ptpn6*-*Ptpn11* and *Chuk*, but not of *Ikbkb*, also blocked TGF-β transcript expression in isolated pDCs (**Fig. 6c**) and abrogated the immunosuppressive ability of TGF-β–conditioned pDCs in an experimental setting of skin test reactivity *in vivo* to the IGRP peptide (containing the prevalent diabetogenic H-$2K^d$-restricted epitope of the islet-specific glucose-6-phosphatase catalytic subunit-related protein) (**Fig. 6d**). Similar loss of immunosuppressive activity of TGF-β–conditioned pDCs was also observed in *Ifnar*$^{-/-}$ mice or following treatment of pDCs with the Fyn inhibitor PP2 (but not negative control PP3) before addition of TGF-β (**Fig. 6d**). In contrast, loss of these genes had no significant effect on the IFN-γ–driven pDC function (**Supplementary Fig. 11**).

Promoter analysis of the mouse TGF-β–encoding gene has revealed that the region contains four noncanonical NF-κB binding sites located at positions –1437, –1319, –1162, and –743 relative to the start of *Tgfb1* transcription. Although the direct

interaction of these promoters with the activator proteins is not formally proven as yet, this observation suggests that NF-κB family members regulates the induction of TGF-β at a transcriptional level. Overall, the data indicate that Fyn-dependent phosphorylation of IDO recruits a variety of downstream signaling effectors—including SHPs and the noncanonical NF-κB pathway—that result in sustained TGF-β production, induction of type I IFNs, and a regulatory pDC phenotype.

IDO induces its own expression

Activation of the noncanonical NF-κB pathway and IFN-α are known to lead to IDO induction in immunoregulatory DCs, including pDCs[9,20,32]. The *Ido1* promoter contains a putative noncanonical NF-κB binding site as well as two ISRE-1/2 (IFN-stimulated response element 1 and 2) elements, which represent binding sites for the transcription factors. We tested the association of noncanonical NF-κB family members and/or IRF3, IRF7[9] and IRF8[33] with the responsive elements in the *Ido1* promoter (**Fig. 7a**). Chromatin immunoprecipitation (ChIP) experiments showed specific binding of p52–RelB dimers and IRF8 to the *Ido1* promoter in pDCs treated with TGF-β, which peaked at 3 and 16 h, respectively.

In pDCs transfected with a plasmid construct containing the mouse *Ido1* promoter upstream of the luciferase gene, IFN-γ induced *Ido1* promoter activity in an intense and rapid (at 3 h) albeit transient fashion (expression returned to basal levels at 16 h; **Fig. 7b**), as previously reported[33]. In response to TGF-β however, the *Ido1* promoter started to be transcriptionally active at 16 h, with high activity even at 48 h **(Fig. 7b)**. The 24-h effect of TGF-β was completely lost in pDCs pretreated with *Ido1*, *Ptpn6*-*Ptpn11*, *Chuk* or *Icsbp1* (encoding IRF8)[33] siRNA or lacking *Ido1* or *Ifnar* expression, whereas no ablating effect could be demonstrated by the use of *Ido2* or *Ikbkb* siRNA or 1-MT (**Fig. 7c**). Longer-term maintenance (up to 48 h) of IDO protein expression (**Fig. 7d**) and enzyme activity (**Fig. 7e**) were also found in pDCs pretreated with TGF-β as compared to IFN-γ, which, however, increased both IDO protein expression and activity but only at early time points (i.e., 24 h). Moreover, TGF-β, but not IFN-γ, effects at 24 h remained measurable after washing the cytokine and incubating cells for an additional 24 h in medium alone (**Fig. 7d,e**). These data suggested that IDO-dependent signaling results in sustained *Ido1* expression in pDCs.

TGF-β conditioning induces long-term tolerance *in vivo*

To clearly discriminate the IFN-γ (acute) *vs.* TGF-β (long-term) effects on IDO regulation, we performed skin test reactivity experiments using pDCs conditioned with either cytokine at late time points. The immunosuppressive effects of TGF-β, but not IFN-γ, pretreatment in pDCs were still detectable at one (data not shown) and three months (**Fig. 8a**). Histological examination showed that, in recipients of TGF-β–conditioned pDCs, the local inflammatory reaction was very limited (data not shown**).** In these mice, $CD4^+Foxp3^+$ cells were present in the popliteal lymph nodes draining the experimental footpads (**Fig. 8b and Supplementary Fig. 12**), and unfractionated $CD4^+$ cells failed to produce IFN-γ when restimulated *in vitro* with specific antigen (**Fig. 8c**). *In vitro,* cocultures of TGF-β–conditioned pDCs and $CD4^+$ T cells, in the presence or in the absence of anti–TGF-β, showed that the emergence of $CD4^+Foxp3^+$ T cells depended on TGF-β, while maintenance of this regulatory population was not. Late addition (i.e., at 48 h) of anti–TGF-β did not reverse Foxp3 expression, indicating that, once induced, the regulatory population is not absolutely contingent on TGF-β (**Fig. 8d** and data not shown).

Therefore, under appropriate environmental conditions, IDO can activate a long-term immunoregulatory circuitry involving control of its own expression, either directly or via modulatory cytokines including TGF-β and type I IFNs[34].

DISCUSSION

Initially identified as a counter-regulatory mechanism in acute inflammation[35] and for its role in feto-maternal tolerance[36], IDO is also critical in balancing inflammation with tolerance in autoimmunity, transplantation and cancer[8,9]. While acute responses are best controlled by the IFN-γ–IDO axis[37,38], TGF-β is critical in establishing a regulatory phenotype in pDCs which enables those cells to generate and sustain the function of T_{reg} cells through the combined effects of tryptophan starvation and kynurenines acting via the aryl hydrocarbon receptor of T cells[13,39,40].

The definition of the crystal structure of human IDO has revealed a folding into a catalytic large C-terminal domain, a noncatalytic small N-terminal domain, and a long loop connecting the two domains. Apart from covering the top of the heme-binding site, the role of the noncatalytic small domain has been unclear. By mapping the human IDO structure, we found that the putative ITIM1 and ITIM2 corresponding to mouse IDO, though spanning quite distant portions of the primary IDO sequence, are positioned very close to each other in an exposed surface region of the protein. In particular, ITIM1 and ITIM2 are positioned in the small domain and in the interconnecting loop, respectively. Alignment of human, dog, rat, and mouse IDO proteins indicated that ITIM1 and ITIM2 sequences are well conserved in those mammals.

Evolution has produced an astonishing variety of novel adaptations in protein functions, but there are some general principles, among which is recruitment of proteins with existing functions for new purposes. The stability of proteins depends on the presence of particular motifs that make them a target of degradative or protective processes. These regulatory signals usually consist of short simple sequence patterns, including evolutionarily conserved ITIMs[41], and new phenotypes can be generated using cryptic phenotypes, as is the case for IDO2, which contains incomplete, and thus inactive, ITIMs. In gene duplication, one of the two duplicates may acquire new functions while the original functions are maintained by the other. Seen in this light, the ITIMs in IDO do not only control the stability of the protein (via ubiquitination and proteasomal degradation driven by IL-6–induced SOCS3)[27], but they also participate in a positive feedback loop operating within a self-maintaining regulatory circuitry in a TGF-β–dominated environment.

Thus, IDO does not only seem critical in limiting potentially exaggerated inflammatory reactions in response to danger signals[11] and in assisting T_{reg} effector

function[9], but also represents an important component of a regulatory system that allows long-term control of immune homeostasis, as may be required by pregnancy[36] and tolerance to self[42]. Central to a continued homeostatic function of the enzyme is its ability to respond to TGF-β in local tissue microenvironment, tip the balance of canonical *vs*. noncanonical NF-κB activation in favor of the latter, and modulate gene transcription so to amplify itself, directly or indirectly via type I IFNs, and maintain a TGF-β–dominated environment. The dual regulatory function of IDO as a catalyst and a signaling protein—that uses, somewhat paradoxically, the same motifs for degradation processes—makes this enzyme one of rare functional eclecticism.

Acknowledgements

This work was supported by the Italian Ministry of Health, project N. GR-2008-1138004 ('Innovative IDO-targeting interventions in autoimmunity'; to C.O.) and in part by Associazione per l'Aiuto ai Giovani con Diabete dell'Umbria (to U.G.) and Associazione Italiana per la Ricerca sul Cancro (to P.P). We thank G. C. Prendergast for the gift of the mIDOprom900-luc plasmid and G. Andrielli for digital art and image editing.

Author Contributions

M.T.P. designed and performed experiments. C.O., C. Volpi, C. Vacca, M.L. B., R.B., C.B., M.C., and E.M.C.M. performed experiments. G.S., S.B., and M.C.F. contributed to experiment design. L.B. and F.G. provided critical reagents. F.F. designed experiments and supervised research. P.P. supervised research. U.G. designed experiments, supervised research, and wrote the manuscript.

METHODS

Methods and any associated references are available in the online version of the paper at http://www.nature.com/natureimmunology/.

Note: Supplementary information is available on the Nature Immunology website.

ONLINE METHODS

Mice, organs, and cell lines. Eight- to ten-week-old female BALB/c (H-2^d) and 129/Sv (H-2^b) mice were obtained from Charles River Breeding Laboratories. B6.129-*Ido1*^{tm1Alm}/J mice, deficient for *Ido1* expression, and B6.Cg-*Foxp3*^{tm2Tch}/J mice, coexpressing the enhanced green fluorescent protein (EGFP) and the regulatory T cell-specific transcription factor Foxp3 under the control of the endogenous promoter, were purchased from The Jackson Laboratory and bred at the animal facilities of the University of Perugia. For both B6.129-*Ido1*^{tm1Alm}/J and B6.Cg-*Foxp3*^{tm2Tch}/J mice, C57BL/6 mice were used as control. Spleens from mice deficient for the IFN-α/β receptor (*Ifnar*$^{-/-}$) and their respective controls on a 129/Sv background were purchased from B & K Universal. Control littermates were included in individual experiments to check for nonspecific effects of each genetic manipulation, and none were found. All *in vivo* studies were in compliance with National (Italian Parliament DL 116/92) and Perugia University Animal Care and Use Committee guidelines.

Reagents. Rabbit monoclonal anti-mouse IDO antibody (cv152) was as described[11]. Rabbit polyclonal anti–phospho-IDO (anti–p-IDO) antibody was raised in our laboratory to a synthetic tyrosine-phosphorylated peptide of 20 amino acids (EGLLpYEGVWDTPKMFSGGSC; purchased from Genemed Synthesis) containing the IDO ITIM2 sequence. The peptide was conjugated to maleimide-activated keyhole limpet hemocyanin (Pierce) through the free C-terminal cysteine residue. Anti–p-IDO antibody specifically recognized the phosphorylated ITIM2 peptide in ELISA and a band corresponding to the IDO size (~45 kDa) on Western blot analysis using lysates from P1 transfectant cells treated for 10 min with Na_3VO_4 (a phosphatase inhibitor) and expressing wild-type IDO but not the IDO.ITIM2 mutant lacking Y_{253}. Anti-Flag M2 antibody was purchased from Sigma-Aldrich. Anti–SHP-1, anti–SHP-2, and anti-SHIP were from Santa Cruz Biotechnology. Antibodies to phospho-IKKα/β, IKKα, and IKKβ were from Cell Signaling. Anti-Fyn and anti-IRAK1 antibodies were also from Cell Signaling. Biotinylated phosphorylated and unphosphorylated peptides for pull-down experiments spanning the ITIM-contained tyrosines of mouse IDO (ITIM1: SGSGNIAVPY$_{115}$CELSE; pITIM1: SGSGNIAVPpY$_{115}$CELSE; ITIM2: SGSGPEGLLY$_{254}$EGVWD; pITIM2: SGSGPEGLLpY$_{253}$EGVWD) were purchased from Sigma-Genosys. The IDO inhibitor 1-MT (D,L-isomers) and the SHP-1 inhibitor sodium stibogluconate were purchased from Sigma-Aldrich. SIS3, a specific inhibitor of TGF-β1/ALK-5 phosphorylation of Smad3, was obtained from Sigma-Aldrich. The Syk inhibitor was purchased from Calbiochem. LY294002 (PI3K inhibitor) was from Cell Signaling Technology. The Fyn inhibitor 3-(4-

chlorophenyl)1-(1,1-dimethyl)-1*H*-pyrazolo[3,4-d]pyrimidin-4-amine (PP2) and its negative control 1-phenyl-1*H*-pyrazolo[3,4-*d*]pyrimidin-4-amine (PP3) were from Tocris Bioscience.

DC purification and treatments. All of these procedures are as described[19,27,37,42]. pDCs were exposed to 200 U/ml IFN-γ or 20 ng/ml TGF-β for 24 hours at 37 °C, unless specifically indicated. For TGF-β neutralization, pDCs were incubated with 1D11 mAb (40 μg/ml). Also used, in specific *in vitro* experiments, were 1-MT (4 μM), sodium stibogluconate (10 μg/ml), SIS3 (5 μM), LY294002 (25 μM), PP2 (5 μM), or PP3 (5 μM) 1 h prior to cytokine treatment. For silencing *Ido1*, *Ido2*, *Chuk* (alias *IKKα*), *Ikbkb* (alias *IKKβ*), *Ptpn6*, *Ptpn11*, *Irak1*, and *Icsbp1*[33]mRNAs, gene-specific siRNA were predesigned on the basis of the respective gene sequence and synthesized by Ambion, which also supplied Negative Control siRNA. In order to exclude possible off-target effects of siRNAs, *Ido1* and *Irak1* silencing were corroborated by the use of an additional reagent, i.e., ON-TARGET*plus* siRNA, which was predesigned on the basis of gene ID 15930 (*Ido1*) or 16179 (*Irak1*) sequence and synthesized by Thermo Scientific (Dharmacon RNAi Technologies). When both *Ido1*- and *Irak1* specific siRNA reagents were used in the same experiment, the Ambion's reagent was designated as *Ido1*-1 or *Irak1*-1 siRNA and the Dharmacon's as *Ido1*-2 or *Irak1*-2 siRNA. Transfection of pDCs was carried out as described[20].

Cytofluorimetric analyses and suppression assay. Purification of naive $CD4^+CD25^-$ T cells from pooled lymph nodes was conducted as described[20,39,43]. For the suppression assay, naive $CD4^+CD25^-$ cells (2×10^5) were cocultured for 3 d with different numbers of $CD4^+$ cells purified from 6-d T cell-pDC cocultures in the presence of 1 μg/ml soluble anti-CD3[19,39,43]. Proliferation was measured by incorporation of [^{3}H]thymidine, according to standard procedures.

ELISA. Mouse cytokines (IL-4, IL-6, IL-10, IL-17A, IL-27 p28, IFN-α, IFN-β, IFN-γ, and TGF-β1) were measured in culture supernatants by ELISA using specific kits (R&D Systems and Abnova Corporation) or previously described reagents and procedures[44]. An ELISA-based TransAM Flexi NF-κB Family Kit (Active Motif) was used to monitor activity of NF-κB family members, as described[20,43].

Skin test assay and histology. A skin test assay was used for measuring class I-restricted delayed-type hypersensitivity in response to intrafootpad challenge with synthetic peptides, as previously described[19,45]. For TGF-β neutralization, recipient mice were treated twice with 0.5 mg of 1D11 mAb 24 h before and after sensitization with pDCs. The response to intrafootpad

challenge with the eliciting peptide was measured at 2 weeks (or at 1–3 months in experiments aimed at evaluating long-term tolerogenic effects), and results were expressed as the increase in footpad weight of peptide-injected footpads over that of respective, vehicle-injected counterparts[19].

Real-Time PCR. Real-time PCR analysis was performed, as described[12,43], using primers specific for *Foxp3*, *Tgfb1*, *Ptpn6*, *Ptpn11*, and *Inpp5d*. In all panels, bars represent the ratio of gene to *Gapdh* expression, as determined by the relative quantification method (ΔΔ cycle threshold; means ± s.d. of triplicate determinations).

Construction and expression of mouse IDO, IDO mutants, and IDO2. Constructs expressing Flag-tagged proteins were generated amplifying the cDNA from cDCs stimulated with IFN-γ (for the *Ido1* gene) or liver cells obtained from mice challenged with *Pseudomonas aeruginosa*[46] (for *Ido2*) with primers containing *Spe*I (sense) and *Not*I (antisense) restriction enzyme site sequences. Antisense primers also contained an N-terminal Flag-encoding sequence and a linker sequence coding for Gly_3 to ensure flexibility of the resulting fusion protein[47]. *Ido1* mutants were obtained by means of crossover PCR using primers containing specific substitutions.

Immunoprecipitation, peptide pull-down experiments, and immunoblot analyses. These procedures were conducted as described[27].

Meta-analysis of pDC gene expression data. To evaluate the expression of a set of tyrosine kinases in untreated mouse pDCs, different gene expression datasets were downloaded from Gene Expression Omnibus (http://www.ncbi.nlm.nih.gov/GEO/) using A-MADMAN (Annotation-based MicroArray Data Meta ANalysis tool[48]; http://xlabserver4.biomed.unimo.it/amadman/) as previously described[44].

ChIP. ChIP was performed using the ChIP assay kit, following manufacturer's instructions (EZ-ChIP Millipore, Upstate Biotechnology). To determine the identity of the target genes, ChIP DNA was analyzed by Real-Time PCR as above. Genomic DNA or input DNA was used as a positive control. The following primer sets were used: *Ido1* promoter ISRE-1 site (sense, 5'-GAGAATCTCCAGGTGGGCAG-3'; antisense, 5'-GACACACAGGAGAGTCAGCC -3'); *Ido1* promoter ISRE-2 site (sense, 5'-TTGGCACTGGGAAGCTGAGGC-3'; antisense, 5'-TTGCTGTCTACTCCACTGACCC-3'); *Ido1* promoter putative noncanonical NF-κB site (sense, 5'-

TAGTCCCTCAACTTAGTGGTCC-3'; antisense, 5'-TGATTTATTCTTGGTGCTGGGTG-3'). The PCR products were then analyzed on 2% agarose gels.

Phosphatase Assay. The phosphatase assay on phosphotyrosine peptide was done using the phosphatase assay kit from Sigma-Aldrich and according to the manufacturer's procedure.

Luciferase and kynurenine assays. pDCs (1×10^7) were electroporated (230 V, 75 Ohm and 1,500 microfarads) in Optimem/Glutamax (Invitrogen) with 30 μg of the mIDOprom900-luc plasmid[49], which contains the mouse *Ido1* promoter (900 bp) and 70 nucleotides of noncoding sequence in *Ido1* exon 1 upstream of the firefly luciferase coding sequence. Another reporter plasmid, pRL-TK (1 μg; Promega) encoding *Renilla* luciferase, was electroporated as an internal control of the transfection process. Luciferase assays were performed using the dual luciferase reporter assay kit (Promega). IDO functional activity was measured *in vitro* in terms of the ability to metabolize tryptophan to L-kynurenine whose concentration was measured by high-performance liquid chromatography in culture supernatants at different times after adding 100 μM tryptophan for 8 h[11,37].

Statistical analysis. Student's *t*-test was used to analyze the results of *in vitro* studies in which data are mean values (± s.d.). In the *in vivo* skin test assay, statistical analysis was performed using two-tailed paired *t*-test by comparing the mean weight of experimental footpads with that of control, saline injected counterparts[50]. Data are mean values (± s.d.) of three experiments with at least six mice per group per experiment, as computed by power analysis to yield a power of at least 80% with an α level of 0.05[20].

References

1. Fazekas de St Groth, B. The evolution of self-tolerance: a new cell arises to meet the challenge of self-reactivity. *Immunol. Today* **19**, 448–454 (1998).
2. Flajnik, M.F. & Kasahara, M. Origin and evolution of the adaptive immune system: genetic events and selective pressures. *Nat. Rev. Genet.* **11**, 47–59 (2010).
3. Grohmann, U. & Bronte, V. Control of immune response by amino acid metabolism. *Immunol. Rev.* **236**, 243–264 (2010).
4. Jeffery, C.J. Moonlighting proteins–an update. *Mol. Biosyst.* **5**, 345–350 (2009).
5. Forouhar, F. *et al.* Molecular insights into substrate recognition and catalysis by tryptophan 2,3-dioxygenase. *Proc. Natl. Acad. Sci. U S A* **104**, 473–478 (2007).
6. Ball, H.J., Yuasa, H.J., Austin, C.J., Weiser, S. & Hunt, N.H. Indoleamine 2,3-dioxygenase-2; a new enzyme in the kynurenine pathway. *Int. J. Biochem. Cell. Biol.* **41**, 467–471 (2009).
7. Metz, R. *et al.* Novel tryptophan catabolic enzyme IDO2 is the preferred biochemical target of the antitumor indoleamine 2,3-dioxygenase inhibitory compound D-1-methyl-tryptophan. *Cancer Res.* **67**, 7082–7087 (2007).
8. Mellor, A.L. & Munn, D.H. IDO expression by dendritic cells: tolerance and tryptophan catabolism. *Nat. Rev. Immunol.* **4**, 762–774 (2004).
9. Puccetti, P. & Grohmann, U. IDO and regulatory T cells: a role for reverse signalling and non-canonical NF-κB activation. *Nat. Rev. Immunol.* **7**, 817–823 (2007).
10. Grohmann, U., Fallarino, F. & Puccetti, P. Tolerance, DCs and tryptophan: much ado about IDO. *Trends Immunol.* **24**, 242–248 (2003).
11. Romani, L. *et al.* Defective tryptophan catabolism underlies inflammation in mouse chronic granulomatous disease. *Nature* **451**, 211–215 (2008).
12. Belladonna, M.L. *et al.* Cutting edge: Autocrine TGF-β sustains default tolerogenesis by IDO-competent dendritic cells. *J. Immunol.* **181**, 5194–5198 (2008).
13. Belladonna, M.L., Orabona, C., Grohmann, U. & Puccetti, P. TGF-β and kynurenines as the key to infectious tolerance. *Trends Mol. Med.* **15**, 41–49 (2009).
14. Irla, M. *et al.* MHC class II-restricted antigen presentation by plasmacytoid dendritic cells inhibits T cell-mediated autoimmunity. *J. Exp. Med.* **207**, 1891–1905 (2010).
15. Matta, B.M., Castellaneta, A. & Thomson, A.W. Tolerogenic plasmacytoid DC. *Eur. J. Immunol.* **40**, 2667–2676 (2010).
16. Lande, R. & Gilliet, M. Plasmacytoid dendritic cells: key players in the initiation and regulation of immune responses. *Ann. N. Y. Acad. Sci.* **1183**, 89–103 (2010).
17. Swiecki, M. & Colonna, M. Unraveling the functions of plasmacytoid dendritic cells during viral infections, autoimmunity, and tolerance. *Immunol. Rev.* **234**, 142–162 (2010).
18. Huang, L., Baban, B., Johnson, B.A., 3rd & Mellor, A.L. Dendritic cells, indoleamine 2,3 dioxygenase and acquired immune privilege. *Int. Rev. Immunol.* **29**, 133–155 (2010).

19. Orabona, C. *et al.* CD28 induces immunostimulatory signals in dendritic cells via CD80 and CD86. *Nat. Immunol.* **5**, 1134–1142 (2004).
20. Grohmann, U. *et al.* Reverse signaling through GITR ligand enables dexamethasone to activate IDO in allergy. *Nat. Med.* **13**, 579–586 (2007).
21. Neel, B.G., Gu, H. & Pao, L. The 'Shp'ing news: SH2 domain-containing tyrosine phosphatases in cell signaling. *Trends Biochem. Sci.* **28**, 284–293 (2003).
22. Billadeau, D.D. & Leibson, P.J. ITAMs versus ITIMs: striking a balance during cell regulation. *J. Clin. Invest.* **109**, 161–168 (2002).
23. Ravetch, J.V. & Lanier, L.L. Immune inhibitory receptors. *Science* **290**, 84–89 (2000).
24. Sweeney, M.C. *et al.* Decoding protein-protein interactions through combinatorial chemistry: sequence specificity of SHP-1, SHP-2, and SHIP SH2 domains. *Biochemistry* **44**, 14932–14947 (2005).
25. Orr, S.J. *et al.* CD33 responses are blocked by SOCS3 through accelerated proteasomal-mediated turnover. *Blood* **109**, 1061–1068 (2007).
26. Orr, S.J. *et al.* SOCS3 targets Siglec 7 for proteasomal degradation and blocks Siglec 7-mediated responses. *J. Biol. Chem.* **282**, 3418–3422 (2007).
27. Orabona, C. *et al.* SOCS3 drives proteasomal degradation of indoleamine 2,3-dioxygenase (IDO) and antagonizes IDO-dependent tolerogenesis. *Proc. Natl. Acad. Sci. U S A* **105**, 20828–20833 (2008).
28. Williams, J.C., Wierenga, R.K. & Saraste, M. Insights into Src kinase functions: structural comparisons. *Trends Biochem. Sci.* **23**, 179–184 (1998).
29. Daeron, M., Jaeger, S., Du Pasquier, L. & Vivier, E. Immunoreceptor tyrosine-based inhibition motifs: a quest in the past and future. *Immunol. Rev.* **224**, 11–43 (2008).
30. An, H. *et al.* Phosphatase SHP-1 promotes TLR- and RIG-I-activated production of type I interferon by inhibiting the kinase IRAK1. *Nat. Immunol.* **9**, 542–550 (2008).
31. Hoshino, K. *et al.* IκB kinase-α is critical for interferon-α production induced by Toll-like receptors 7 and 9. *Nature* **440**, 949–953 (2006).
32. Tas, S.W. *et al.* Noncanonical NF-κB signaling in dendritic cells is required for indoleamine 2,3-dioxygenase (IDO) induction and immune regulation. *Blood* **110**, 1540–1549 (2007).
33. Orabona, C. *et al.* Toward the identification of a tolerogenic signature in IDO-competent dendritic cells. *Blood* **107**, 2846–2854 (2006).
34. Puccetti, P. On watching the watchers: IDO and type I/II IFN. *Eur. J. Immunol.* **37**, 876–879 (2007).
35. Taylor, M.W. & Feng, G.S. Relationship between interferon-γ, indoleamine 2,3-dioxygenase, and tryptophan catabolism. *Faseb J.* **5**, 2516–2522 (1991).
36. Munn, D.H. *et al.* Prevention of allogeneic fetal rejection by tryptophan catabolism. *Science* **281**, 1191–1193 (1998).
37. Grohmann, U. *et al.* CTLA-4–Ig regulates tryptophan catabolism *in vivo*. *Nat. Immunol.* **3**, 1097–1101 (2002).
38. Fallarino, F. *et al.* Modulation of tryptophan catabolism by regulatory T cells. *Nat. Immunol.* **4**, 1206–1212 (2003).
39. Fallarino, F. *et al.* The combined effects of tryptophan starvation and tryptophan catabolites down-regulate T cell receptor ζ-chain and induce a regulatory phenotype in naive T cells. *J. Immunol.* **176**, 6752–6761 (2006).

40. Mezrich, J.D. *et al.* An interaction between kynurenine and the aryl hydrocarbon receptor can generate regulatory T cells. *J. Immunol.* **185**, 3190–3198 (2010).
41. Abu-Dayyeh, I. *et al.* Identification of key cytosolic kinases containing evolutionarily conserved kinase tyrosine-based inhibitory motifs (KTIMs). *Dev. Comp. Immunol.* **34**, 481–484 (2010).
42. Grohmann, U. *et al.* A defect in tryptophan catabolism impairs tolerance in nonobese diabetic mice. *J. Exp. Med.* **198**, 153–160 (2003).
43. Fallarino, F. *et al.* IDO mediates TLR9-driven protection from experimental autoimmune diabetes. *J. Immunol.* **183**, 6303–6312 (2009).
44. Fallarino, F. *et al.* Metabotropic glutamate receptor-4 modulates adaptive immunity and restrains neuroinflammation. *Nat. Med.* **16**, 897–902 (2010).
45. Orabona, C. *et al.* Cutting edge: silencing suppressor of cytokine signaling 3 expression in dendritic cells turns CD28-Ig from immune adjuvant to suppressant. *J. Immunol*. **174**, 6582–6586 (2005).
46. Belladonna, M.L. *et al.* IL-23 neutralization protects mice from Gram-negative endotoxic shock. *Cytokine* **34**, 161–169 (2006).
47. Belladonna, M.L. *et al.* IL-23 and IL-12 have overlapping, but distinct, effects on murine dendritic cells. *J. Immunol.* **168**, 5448–5454 (2002).
48. Bisognin, A. *et al.* A-MADMAN: annotation-based microarray data meta-analysis tool. *BMC Bioinformatics* **10**, 201–211 (2009).
49. Muller, A.J., DuHadaway, J.B., Donover, P.S., Sutanto-Ward, E. & Prendergast, G.C. Inhibition of indoleamine 2,3-dioxygenase, an immunoregulatory target of the cancer suppression gene *Bin1*, potentiates cancer chemotherapy. *Nat. Med.* **11**, 312–319 (2005).
50. Grohmann, U. *et al.* Functional plasticity of dendritic cell subsets as mediated by CD40 versus B7 activation. *J. Immunol.* **171**, 2581–2587 (2003).

Figure legends

Figure 1 | IDO catalytic activity is not required for the IDO-dependent, immunoregulatory effects of pDCs conditioned with TGF-β *in vitro.* (**a**) $CD4^+$ T cell proliferation was measured as percentage of EdU^+ cells by cytofluorimetric analysis in 4 day cocultures of $CD4^+CD25^-$ T cells and pDCs either untreated (None) or treated with IFN-γ or TGF-β. pDCs were transfected with a scrambled sequence (Control), one of two distinct *Ido1* siRNA (siRNA-1 and -2; see Methods for details), *Ido2* siRNA, or treated with 1-MT. (**b**) Apoptosis of $CD4^+$ T cells was measured as percentage of PI^+Annexin (Ann) V^+ cells in 24 h cocultures. (**c**) Expression of Foxp3 was assessed by cytofluorimetric analysis as percentage of $CD4^+Foxp3^+$ cells in 4 d cocultures. Data in **a**, **b**, and **c**, are mean values (± s.d.) of three independent experiments. Representative histograms and plots of one experiment in **a**, **b**, and **c** are shown in **Supplementary Figs. 2–4**. (**d**) Proliferation of $CD4^+CD25^-$ T cells cultured in various numbers (horizontal axis) as in **a,** in the presence of soluble anti-CD3 and irradiated T cell-depleted splenocytes. Data are means (± s.d.) of triplicate samples and are from one of three representative experiments. **(e**) Cytokine amounts were measured in supernatants of 4 d cocultures established as in **a**. Data are mean values (± s.d.) of three experiments, each performed in triplicate. (**a**–**e**) $*P < 0.01$ and $**P < 0.001$. (**f**) TGF-β1 expression is shown on $120G8^+$ pDCs from wild-type C57BL/6 (WT) or $Ido^{-/-}$ mice following 24 h of treatment with TGF-β or medium alone (Control). One experiment representative of three is shown [compiled data (mean ± s.d.) for the three experiments are: TGF-β, 4.5 ± 1.5; wild-type control, 1.2 ± 0.4; $P = 0.011$].

Figure 2 | IDO catalytic activity is not required for IDO-dependent, immunoregulatory effects induced *in vivo* by pDCs conditioned with TGF-β. (**a**) *In vivo* suppressive activity of cytokine-conditioned pDCs was evaluated by skin test assay. DCs from C57BL/6 mice were fractionated according to CD8 or mPDCA-1 expression, pulsed with HY, and transferred into B6.Cg-*Foxp3* recipient mice to be assayed for skin reactivity at 15 d to the eliciting peptide. The $CD8^-$ fraction was used alone or in combination with a minority fraction (5%) of pDCs conditioned by IFN-γ or TGF-β. pDCs were used as non-transfected (Control), transfected with negative

control (NC, scrambled sequence), *Ido1*, or *Ido2* siRNA, or treated with 1-MT. Additional groups involved the administration of anti-TGF-β at the time of DC sensitization. (**b**) Histology was done on left (peptide-injected; Experimental footpad) footpad sections from representative mice at 15 d of sensitization and at 24 h of intrafootpad challenge with the peptide or vehicle alone (Control footpad). Sections were stained with hematoxylin and eosin (H&E) to assess leukocyte infiltration. Pictures of original representative footpads are also shown. Scale bar, 100 μm. (**c**) Production of IFN-γ was assessed on leukocytes harvested from PLNs (draining left hind footpads) of mice ($n = 6$ per group) sensitized with peptide-pulsed DCs—untreated (None) or treated with IFN-γ or TGF-β (indicated)—15 d earlier and challenged intrafootpad with HY 24 h before testing. IFN-γ was measured in culture supernatants after cell restimulation *in vitro* with HY for 48 h. (**d**) Expression of Foxp3 was measured as percentage of $CD4^+Foxp3^+$ cells by cytofluorimetric analysis in PLNs harvested as in **c**. (**a**–**d**) $*P < 0.01$ and $**P < 0.001$.

Figure 3 | TGF-β induces the formation of IDO–SHP-1/2 complexes and activation of SHP-1 phosphatase activity in pDCs. (**a**) Kinetics are shown of IDO ITIM2 phosphorylation in pDCs conditioned with TGF-β or IFN-γ. Lysates from pDCs treated with either cytokine were sequentially blotted with anti-pITIM2 (p-IDO), anti-IDO, and β-tubulin–specific antibody. (**b**) Real-Time PCR kinetic analysis is shown of *Ptpn6*, *Ptpn11*, and *Inpp5d* transcript levels in pDCs treated as in **a**. *Gapdh* was used for normalization. Data (means ± s.d. from three experiments) are presented as fold change in normalized transcript expression in cytokine-treated pDCs relative to untreated counterparts (in which fold change = 1; dotted line). (**c**) Pull-down experiments were conducted with phosphorylated IDO peptides. Lysates from untreated P1 cells and TGF-β–treated pDCs were pulled down with unphosphorylated (ITIM1 and ITIM2) or tyrosine-phosphorylated (pITIM1 and pITIM2) IDO peptides and sequentially immunoblotted with anti–SHP-1, –SHP-2, and –SHIP. The same antibodies were also used in parallel Western blot analyses of whole cell lysates (WCL). (**d**) Co-immunoprecipitation data are shown involving anti-IDO. Lysates from pDCs, either untreated or treated with TGF-β for 24 h, were immunoprecipitated with anti-IDO and then sequentially blotted with anti–SHP-1, –SHP-2, and –IDO. Immunoblots of one-tenth WCL aliquots were used as loading controls. (**a**–**d**) One

representative experiment is shown out of three. (**e**) Phosphatase activity was measured in anti–IDO immunoprecipitates from pDCs treated as in **d**. pDCs were also used after transfection with negative control (NC), *Ptpn6*, or *Ptpn11* siRNA or after treatment with stibogluconate (Stibo). Results are expressed as picomoles (mean ± SD from three independent experiments) of free phosphate released in samples of 50 µl. **P* < 0.01 and ***P* < 0.001. (**f**) Data are shown of phosphatase activity co-immunoprecipitated from P1.IDO transfectants (upper panel; with or without Stibo) and kynurenine production by P1.IDO transfectants (lower panel; with or without 4 µM 1-MT). Upper panel, **P* < 0.05 and ***P* < 0.005. Lower panel, **P* < 0.01 and ***P* < 0.001. ND, not detectable. **(g)** Intracellular immunofluorescence colocalization of IDO and SHP-1 was evaluated in P1 cells transfected as in **f**, treated for 10 min with Na_3VO_4, and fixed with formaldehyde. Alexa 488-labeled anti-IDO was used in combination with anti–SHP-1 and Cγ3-conjugated anti-mouse Ig. Nuclei were stained with DAPI (blue). One experiment of three is shown.

Figure 4 | IDO phosphorylation requires PI3K-dependent but Smad-independent TGF-β signaling events and is mediated by Fyn but not Syk kinase. (a) Modulation of IDO ITIM2 phosphorylation was evaluated in pDCs pretreated for 1 h with SIS3 or LY294002 before incubation with TGF-β for 60 min. pDC lysates were sequentially blotted with anti-pITIM2 (p-IDO), anti-IDO, and β-tubulin–specific antibody. (**b**) Real-Time PCR analysis was conducted to assess *Ptpn6* transcript levels in pDCs treated with TGF-β for 16 h with or without SIS3 or LY294002. Values were normalized as in Fig. 3b. **P* < 0.001. (**c**) Distribution is shown of absolute expression levels of genes coding for mouse Src kinases (indicated) in a panel of 17 untreated mouse pDC samples derived from publicly-available gene expression datasets. (**d**) Heat-map depicts relative changes of scaled expression values of genes as in **c** in 17 untreated mouse pDC samples derived from six different GEO series. (**e**) Immunoblot analysis is shown of expression of Fyn in lysates of pDCs treated or not with TGF-β for 24 h. (**f**) Modulation of IDO ITIM2 phosphorylation was evaluated as in **a** in pDCs treated for 1 h with PP2, PP3 or the Syk inhibitor before incubation with TGF-β for 60 min. (**a**,**e**,**f**) One experiment representative of two is shown.

Figure 5 | IDO and SHPs drive a signaling pathway in pDCs that involves activation of noncanonical NF-κB and production of type I IFN. (**a**) Activation of IKKα and IKKβ in cytokine-conditioned pDCs was assessed using lysates from pDCs treated for different times with TGF-β or IFN-γ that were sequentially blotted with anti–p-IKKα/β, anti-IKKα and anti-IKKβ antibody. The expected migrations of p-IKKα, p-IKKβ, are indicated. Blot is representative of three experiments. (**b**) Nuclear translocation was assessed of NF-κB family members in pDCs. An ELISA procedure was used to monitor activation of p65, p52, and RelB in nuclear extracts from pDCs either untreated (None) or treated as in **a** for 30 or 60 min. pDCs were also used after transfection with negative control (NC), *Ido1*, *Ido2*, *Ptpn6*, and/or *Ptpn11* siRNA. Selected samples were instead pretreated with 1-MT for 1 h. Relative activities (A_{450}) are mean ± s.d. of three experiments, each in triplicate. **P* < 0.05 and ***P* < 0.01 (cytokine-treated *vs.* untreated cells). (**c**) IFN-α production was measured in supernatants from BALB/c, C57BL/6, or *Ido1*$^{-/-}$ pDCs treated for 24 h with IFN-γ or TGF-β by ELISA. Two distinct *Ido1* siRNA were used as in **Fig. 1a**. The effects of *Irak1* siRNA and 1-MT were also assayed. A second control *Irak1* siRNA (see Methods) gave results indistinguishable from those of the siRNA shown in the Figure. Data are mean values (± s.d.) of three experiments, each performed in triplicate. **P* < 0.01 and ***P* < 0.001. (**d**) Co-immunoprecipitation of IRAK1 and IDO with SHPs. Lysates from pDCs transfected with the *Ido1*-containing construct, either untreated or treated with TGF-β for 24 h, were immunoprecipitated with a mixture of anti–SHP-1 and –SHP-2 and then sequentially blotted with anti-IDO, anti–IRAK1, anti–SHP-1, and anti–SHP-2. Blots are representative of two experiments.

Figure 6 | IDO-dependent immunoregulatory effects of pDCs conditioned with TGF-β are mediated by Fyn, SHPs, noncanonical NF-κB, and type I IFN signaling. (a) Percentage are shown of $CD4^+Foxp3^+$ cells in cocultures set up with pDCs treated with TGF-β and lacking specific genes. $CD4^+CD25^-$ T cells were cocultured for 4 d with TGF-β–treated pDCs. The latter cells were purified from BALB/c wild-type mice and transfected with different siRNA (indicated) or from wild-type or *Ifnar*$^{-/-}$ 129/Sv mice. Data are mean values (± s.d.) of three experiments. **P* < 0.01. (**b**) IL-6 levels were measured in cocultures established with pDCs lacking specific genes and treated with TGF-β. IL-6 was measured in supernatants from 4-d

cocultures established as in **a**. Data are mean values (± s.d.) of three experiments, each performed in triplicate. (**c**) Real-Time PCR analysis was conducted of *Tgfb1* transcript levels in pDCs transfected with different siRNA (indicated) and treated with TGF-β for 16 h. Values were normalized as in Fig. 3b. (**d**) Modulation of *in vivo* suppressive activity of pDCs treated with TGF-β. The skin test assay was performed as in Fig. 2a. BALB/c pDCs were used as such, after 1 h pretreatment with PP2 or PP3, or after transfection with negative control (NC), *Ptpn6*-*Ptpn11*, *Chuk*, or *Ikbkb* siRNA. Untransfected pDCs purified from wild type (129/Sv) or *Ifnar*$^{-/-}$ 129/Sv mice were also used in combination with the IGRP peptide. (**a**–**d**) **P* < 0.001.

Figure 7 | TGF-β but not IFN-γ induces long-term expression of IDO in pDCs. (**a**) ChIP of p52/RelB, IRF-3, IRF-4 (used as a negative control), IRF-7, and IRF-8 binding to mouse *Ido1* promoter in pDCs treated with TGF-β for 3 h (p52–RelB) or 16 h (IRFs) was quantified by means of Real-Time PCR using primers comprising the putative noncanonical NF-κB, ISRE-1, or ISRE-2 binding region. Values were normalized as in **Fig. 3b**. (**b**) Time course of activation is shown of the *Ido1* promoter. pDCs were transfected with the mIDOprom900-luc construct and incubated with IFN-γ or TGF-β for 3–48 h. Data (means ± s.d. from three experiments each performed in triplicate) are presented as fold change in luciferase activity (normalized to the activity of a cotransfected constitutive reporter) in cytokine-treated pDCs relative to untreated counterparts (in which fold change = 1; dotted line). (**c**) *Ido1* promoter activity was assessed in pDCs lacking specific genes. Wild-type BALB/c, wild-type (129/Sv) or *Ifnar*$^{-/-}$ 129/Sv, wild-type (C57BL/6) or *Ido1*$^{-/-}$ pDCs were used as non-transfected (None), transfected with negative control (NC, scrambled sequence), or transfected with gene-specific siRNA (indicated) prior to incubation with TGF-β for 24 h. Two distinct *Ido1* siRNA were used as in **Fig. 1a**. Luciferase activity of the mIDOprom900-luc construct was assessed as in **b**. (**d**) Time course of IDO protein expression is depicted. Lysates from pDCs incubated with TGF-β or IFN-γ for 24-48 h were sequentially blotted with anti-IDO and anti–β-tubulin. In selected samples, cells were incubated with medium alone for 24 h after a 24-h treatment with the cytokine and extensive washes (w). One experiment of three. (**e**) Time-course of IDO catalytic activity is shown. pDCs were untreated (None) or treated with IFN-γ or TGF-β for 16–48 h and kynurenine concentrations (mean ± s.d.

of three experiments, each in triplicate) were measured in culture supernatants. Selected samples (Wash) were treated as in **d**. **P* < 0.01.

Figure 8 | pDCs conditioned by TGF-β but not IFN-γ exert long-term immunoregulatory effects *in vivo*. (**a**) Long-term skin test assay involved combinations of HY-pulsed (C57BL/6 or *Ido1*$^{-/-}$) CD8^{-} DCs and pDCs, the latter being untreated (None) or pretreated with either IFN-γ or TGF-β for 24 h, using B6.Cg-*Foxp3* (for C57BL/6 pDCs) or C57BL/6 (for both C57BL/6 and *Ido1*$^{-/-}$ pDCs) recipients. The skin test assay was performed at 3 months. **P* < 0.001. (**b**) Expression of Foxp3 was measured as percentage of CD4^{+}Foxp3^{+} cells by cytofluorimetric analysis in leukocytes harvested from PLNs (draining left hind footpads) of mice (*n* = 6 per group) sensitized as in **a** with peptide-pulsed DCs three months earlier and challenged intrafootpad with the peptide 24 h before. (**c**) Production of IFN-γ was measured using PLN leukocytes harvested as in **b** after restimulation *in vitro* with HY for 48 h. (**a**–**c**) **P* < 0.01 and ***P* < 0.001. (**d**) The effect of the anti–TGF-β—added at the beginning (time 0) or at 48 h to cocultures of CD4^{+}CD25^{-} T cells and pDCs either untreated (None) or treated with IFN-γ or TGF-β—was measured as percentage of CD4^{+}Foxp3^{+} cells by cytofluorimetric analysis at 4 d of culture. One experiment representative of two is shown.

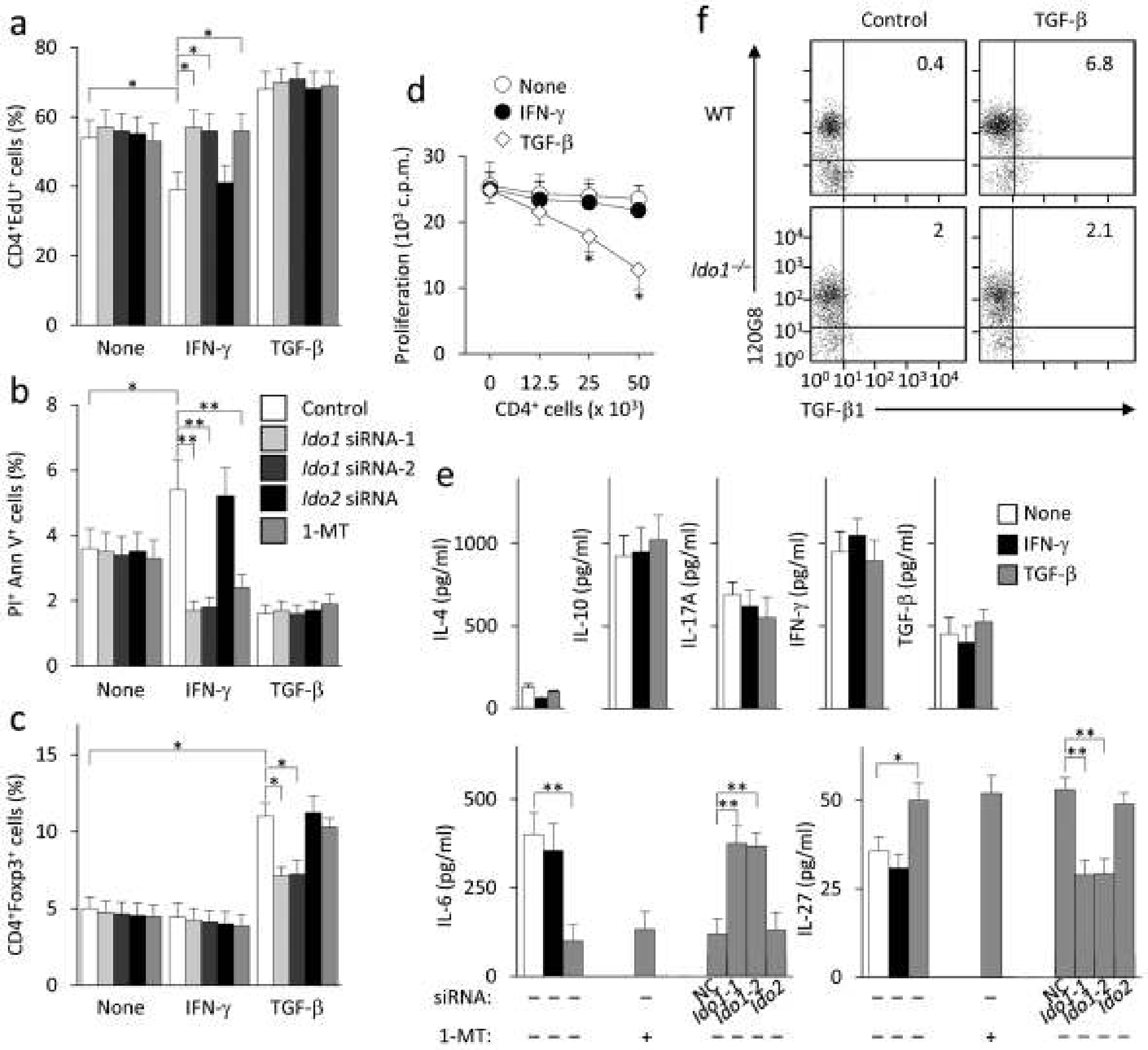
a
CD4+EdU+ cells (%)
None
IFN-γ
TGF-β
b
PI+ Ann V+ cells (%)
Control
Ido1 siRNA-1
Ido1 siRNA-2
Ido2 siRNA
1-MT
c
CD4+Foxp3+ cells (%)
d
None
IFN-γ
TGF-β
Proliferation (10³ c.p.m.)
CD4+ cells (x 10⁵)
e
IL-4 (pg/ml)
IL-10 (pg/ml)
IL-17A (pg/ml)
IFN-γ (pg/ml)
TGF-β (pg/ml)
IL-6 (pg/ml)
IL-27 (pg/ml)
siRNA:
1-MT:
NC
Ido1-1
Ido1-2
Ido2
f
Control
TGF-β
WT
Ido1-/-
120G8
TGF-β1
0.4
6.8
2
2.1

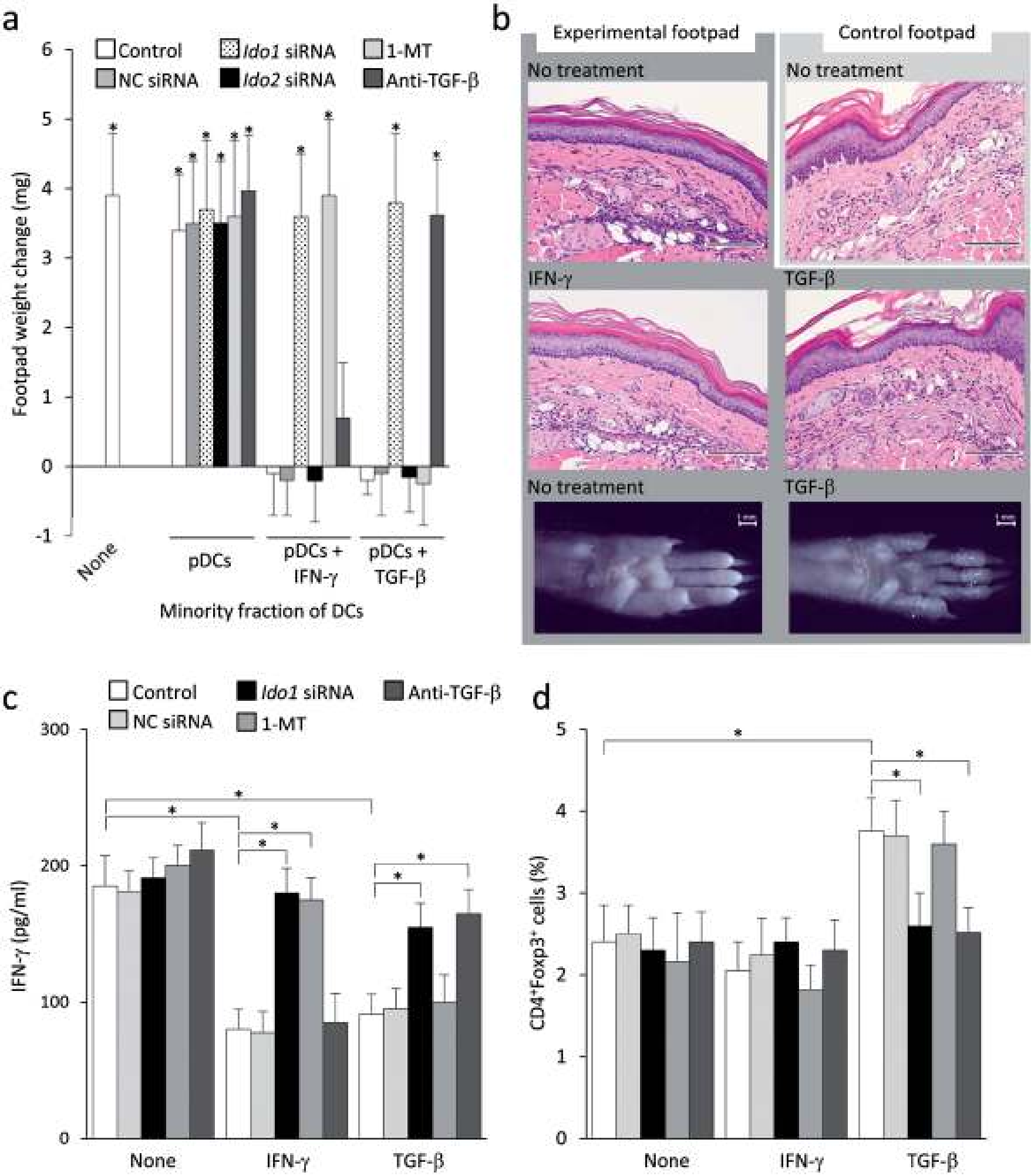
a
Control
NC siRNA
Ido1 siRNA
Ido2 siRNA
1-MT
Anti-TGF-β
Footpad weight change (mg)
6
5
4
3
2
1
0
-1
None
pDCs
pDCs + IFN-γ
pDCs + TGF-β
Minority fraction of DCs
b
Experimental footpad
Control footpad
No treatment
No treatment
IFN-γ
TGF-β
No treatment
TGF-β
c
Control
NC siRNA
Ido1 siRNA
1-MT
Anti-TGF-β
IFN-γ (pg/ml)
300
200
100
0
None
IFN-γ
TGF-β
d
CD4+Foxp3+ cells (%)
5
4
3
2
1
0
None
IFN-γ
TGF-β

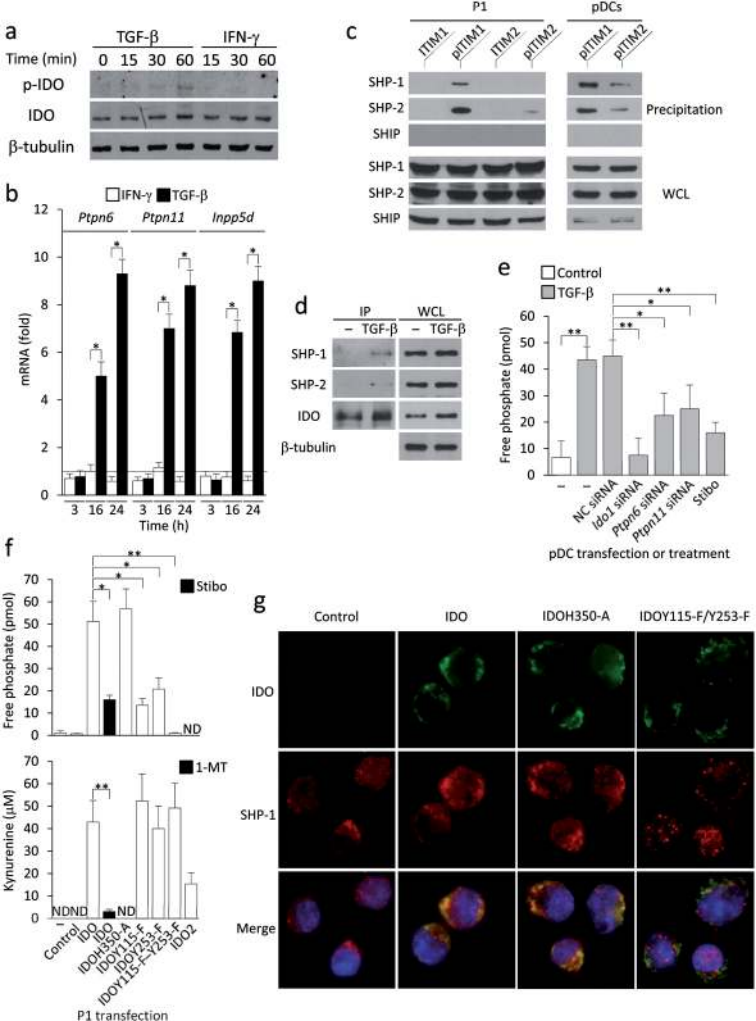
a
TGF-β
IFN-γ
Time (min)
0 15 30 60 15 30 60
p-IDO
IDO
β-tubulin
b
IFN-γ
TGF-β
Ptpn6
Ptpn11
Inpp5d
mRNA (fold)
3 16 24 3 16 24 3 16 24
Time (h)
c
P1
pDCs
ITIM1
pITIM1
ITIM2
pITIM2
pITIM1
pITIM2
SHP-1
SHP-2
SHIP
Precipitation
WCL
d
IP
WCL
– TGF-β
SHP-1
SHP-2
IDO
β-tubulin
e
Control
TGF-β
Free phosphate (pmol)
– – NC siRNA Ido1 siRNA Ptpn6 siRNA Ptpn11 siRNA Stibo
pDC transfection or treatment
f
Stibo
Free phosphate (pmol)
ND
1-MT
Kynurenine (μM)
NDND ND
Control – IDO IDO IDOH350-A IDOY115-F IDOY253-F IDOY115-F/Y253-F IDO2
P1 transfection
g
Control
IDO
IDOH350-A
IDOY115-F/Y253-F
IDO
SHP-1
Merge

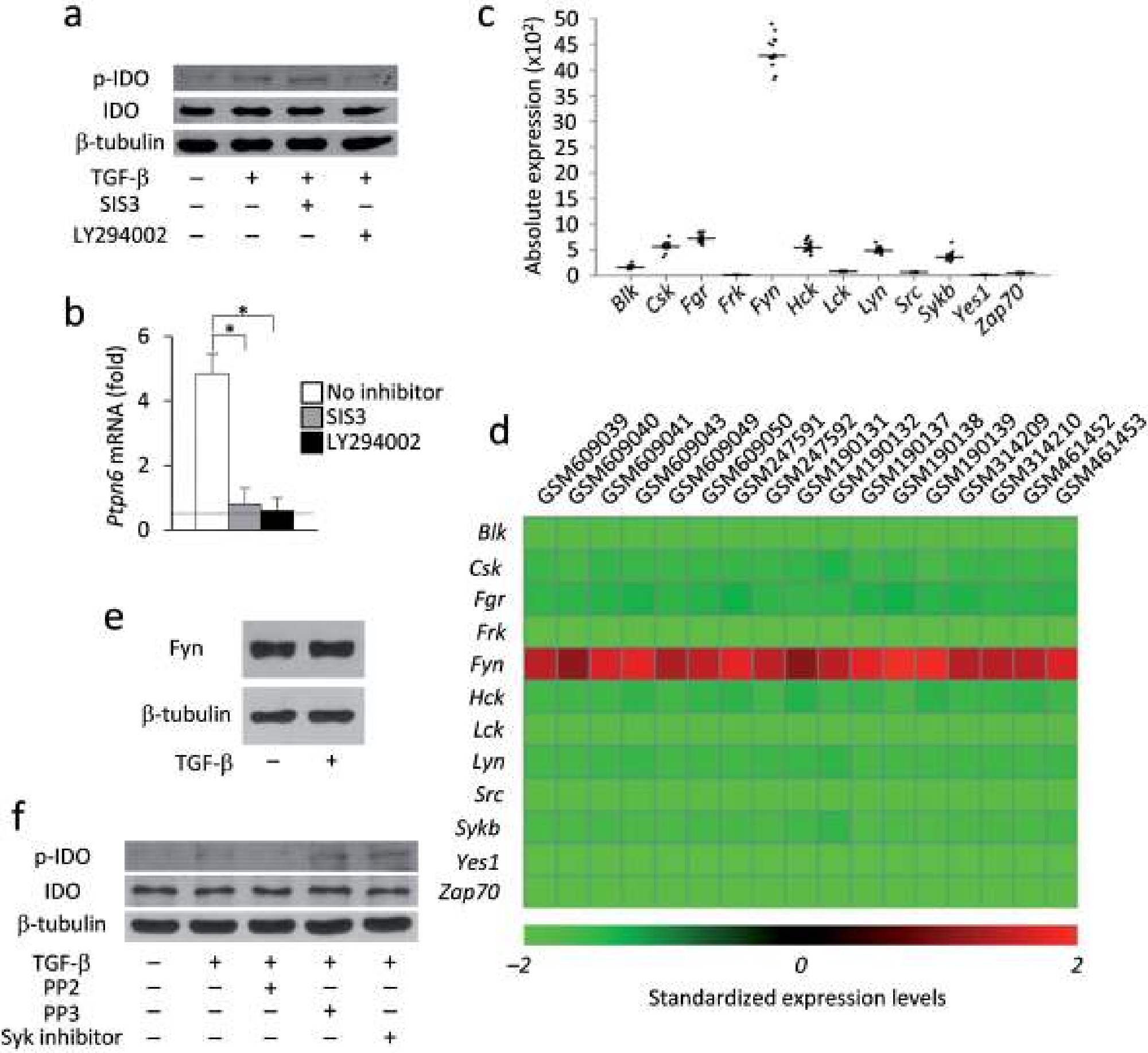
a
p-IDO
IDO
β-tubulin
TGF-β – + + +
SIS3 – – + –
LY294002 – – – +
b
Ptpn6 mRNA (fold)
No inhibitor
SIS3
LY294002
c
Absolute expression (x10²)
Blk Csk Fgr Frk Fyn Hck Lck Lyn Src Sykb Yes1 Zap70
d
GSM609039 GSM609040 GSM609041 GSM609043 GSM609049 GSM609050 GSM247591 GSM247592 GSM190131 GSM190132 GSM190137 GSM190138 GSM190139 GSM3314209 GSM3314210 GSM461452 GSM461453
Blk
Csk
Fgr
Frk
Fyn
Hck
Lck
Lyn
Src
Sykb
Yes1
Zap70
−2 0 2
Standardized expression levels
e
Fyn
β-tubulin
TGF-β – +
f
p-IDO
IDO
β-tubulin
TGF-β – + + + +
PP2 – – + – –
PP3 – – – + –
Syk inhibitor – – – – +

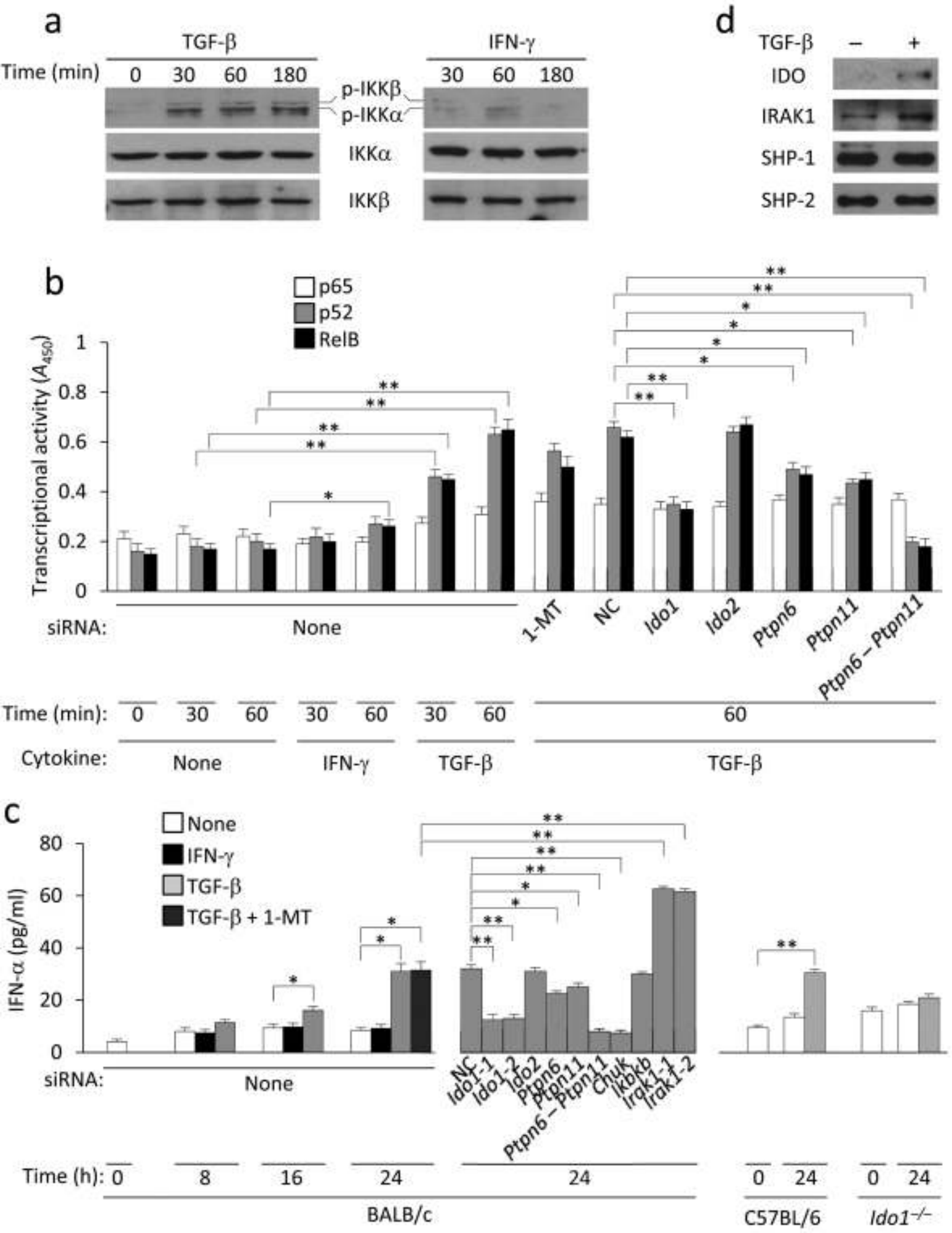
a
TGF-β
IFN-γ
Time (min)
0
30
60
180
30
60
180
p-IKKβ
p-IKKα
IKKα
IKKβ
d
TGF-β
–
+
IDO
IRAK1
SHP-1
SHP-2
b
p65
p52
RelB
Transcriptional activity (A_{450})
1
0.8
0.6
0.4
0.2
0
siRNA:
None
1-MT
NC
Ido1
Ido2
Ptpn6
Ptpn11
Ptpn6 – Ptpn11
Time (min):
0
30
60
30
60
30
60
60
Cytokine:
None
IFN-γ
TGF-β
TGF-β
c
None
IFN-γ
TGF-β
TGF-β + 1-MT
IFN-α (pg/ml)
80
60
40
20
0
siRNA:
None
NC
Ido1-1
Ido1-2
Ido2
Ptpn6
Ptpn11
Ptpn6 – Ptpn11
Chuk
Ikbkb
Irgk1-1
Irak1-2
Time (h):
0
8
16
24
24
0
24
0
24
BALB/c
C57BL/6
Ido1−/−

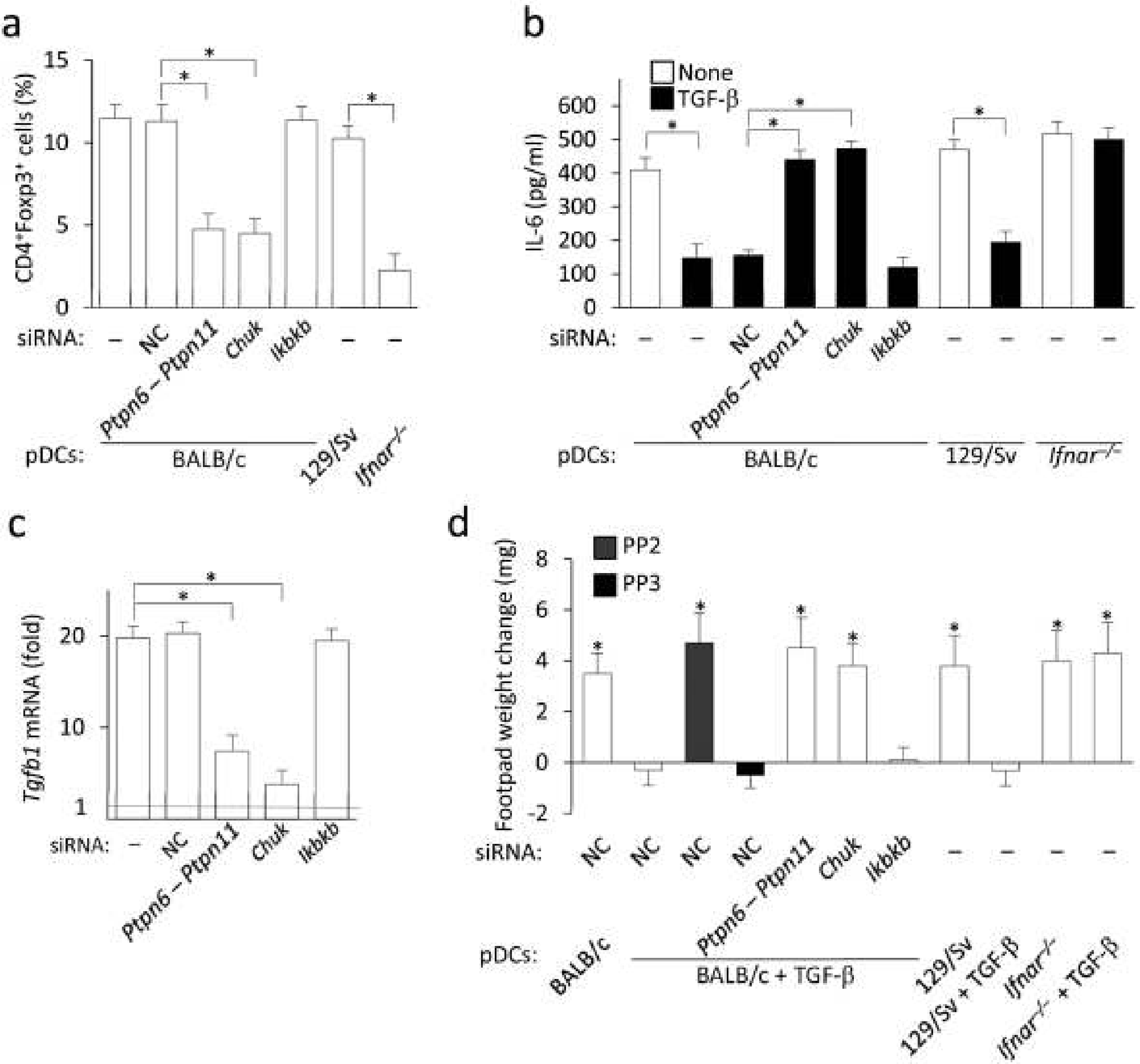
a
CD4+Foxp3+ cells (%)
15
10
5
0
*
*
*
siRNA:
–
NC
Ptpn6 – Ptpn11
Chuk
Ikbkb
–
–
pDCs:
BALB/c
129/Sv
Ifnar−/−
b
None
TGF-β
IL-6 (pg/ml)
600
500
400
300
200
100
0
*
*
*
*
siRNA:
–
–
NC
Ptpn6 – Ptpn11
Chuk
Ikbkb
–
–
–
–
pDCs:
BALB/c
129/Sv
Ifnar−/−
c
Tgfb1 mRNA (fold)
20
10
1
*
*
*
siRNA:
–
NC
Ptpn6 – Ptpn11
Chuk
Ikbkb
d
PP2
PP3
Footpad weight change (mg)
8
6
4
2
0
-2
*
*
*
*
*
*
*
siRNA:
NC
NC
NC
NC
Ptpn6 – Ptpn11
Chuk
Ikbkb
–
–
–
–
pDCs:
BALB/c
BALB/c + TGF-β
129/Sv
129/Sv + TGF-β
Ifnar−/−
Ifnar−/− + TGF-β

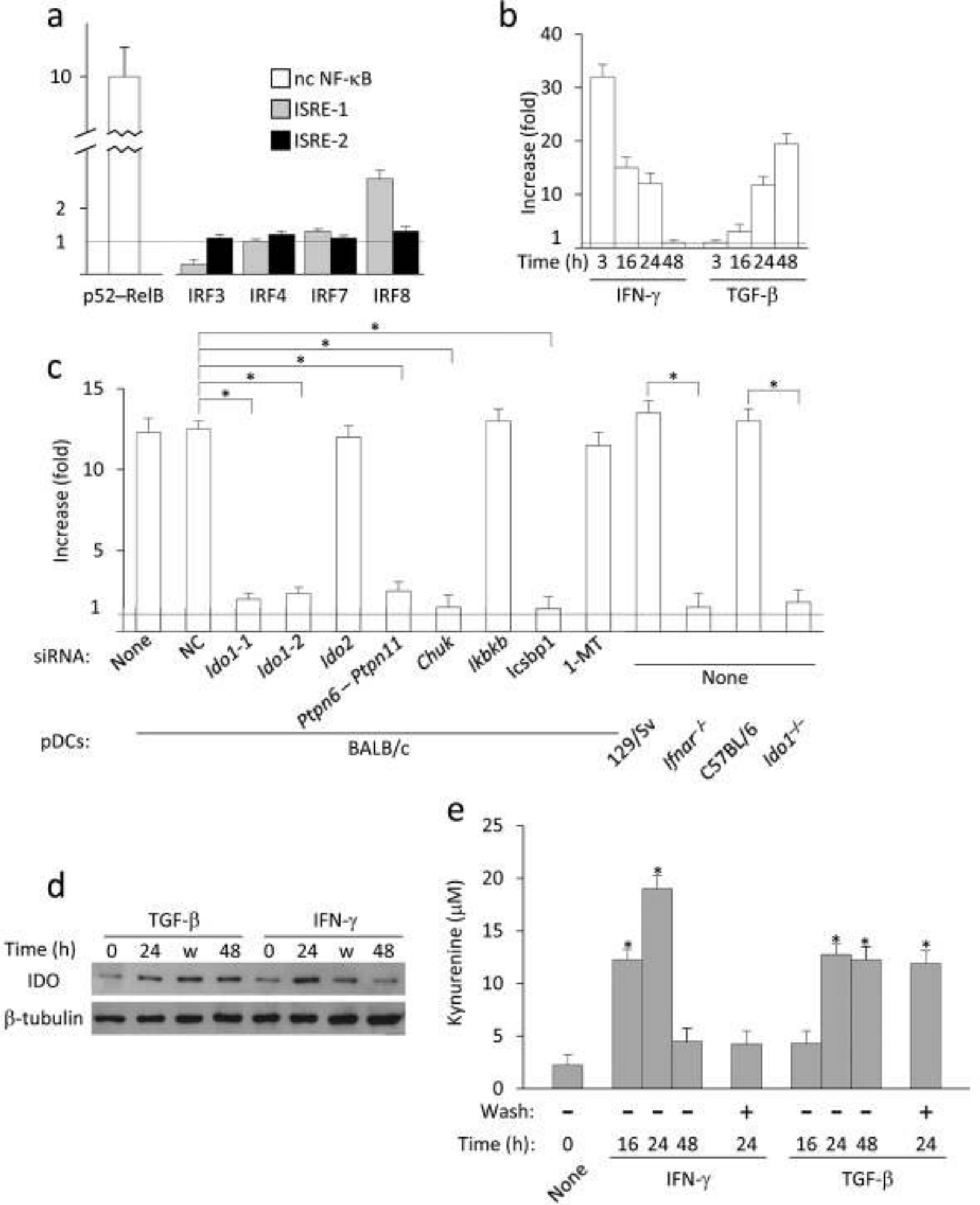
a
10
2
1
nc NF-κB
ISRE-1
ISRE-2
p52–RelB
IRF3
IRF4
IRF7
IRF8
b
40
30
20
10
1
Increase (fold)
Time (h) 3 16 24 48 3 16 24 48
IFN-γ
TGF-β
c
15
10
5
1
Increase (fold)
*
siRNA: None NC Ido1-1 Ido1-2 Ido2 Ptpn6 – Ptpn11 Chuk Ikbkb Icsbp1 1-MT None
pDCs: BALB/c 129/Sv Ifnar-/- C57BL/6 Ido1-/-
d
TGF-β
IFN-γ
Time (h) 0 24 w 48 0 24 w 48
IDO
β-tubulin
e
25
20
15
10
5
0
Kynurenine (μM)
Wash: - - - - + - - - +
Time (h): 0 16 24 48 24 16 24 48 24
None
IFN-γ
TGF-β

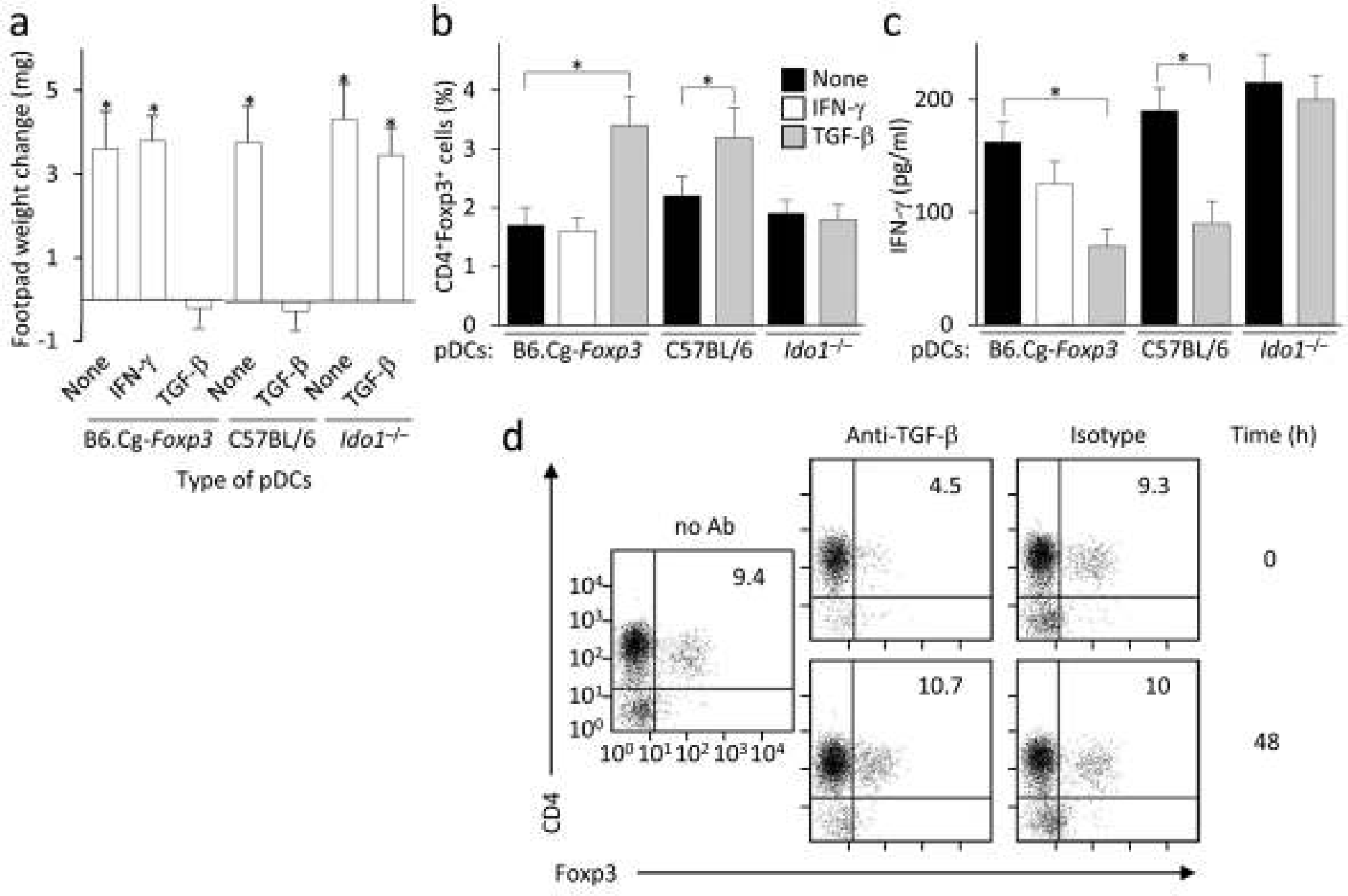
a
Footpad weight change (mg)
5
3
1
-1
None
IFN-γ
TGF-β
None
TGF-β
None
TGF-β
B6.Cg-Foxp3
C57BL/6
Ido1−/−
Type of pDCs
b
CD4+Foxp3+ cells (%)
4
3
2
1
0
None
IFN-γ
TGF-β
pDCs:
B6.Cg-Foxp3
C57BL/6
Ido1−/−
c
IFN-γ (pg/ml)
200
100
0
pDCs:
B6.Cg-Foxp3
C57BL/6
Ido1−/−
d
Anti-TGF-β
Isotype
Time (h)
no Ab
9.4
4.5
9.3
10.7
10
0
48
CD4
Foxp3
10⁰ 10¹ 10² 10³ 10⁴